

LAWS GOVERNING THE MOTION OF GAS BUBBLES
IN A FLUIDIZED BED

A. I. Tamarin, Yu. S. Teplitskii,
and Yu. E. Livshits

UDC 532.546

The diameters of gas bubbles in an inhomogeneous fluidized bed are determined experimentally. A model is proposed, on the basis of which the known experimental data on bubble growth in such a system are generalized.

The behavior of technological processes in a fluidized bed is determined largely by the hydrodynamic phase and inhomogeneities (gas bubbles) formed in the system. A wealth of experimental data has been compiled to date on the motion of gas bubbles, and some partial correlations have been obtained [1, 4, 8]. So far, however, the fundamental laws of growth and motion of gas bubbles in a fluidized bed remain unclear, making it difficult to formulate analytical hydrodynamic models of the system.

We have attempted to gather data on the motion of gas bubbles in a fluidized bed and to explain the general laws governing their development.

In a fluidized bed the energy of the gas filtered through the bed is dissipated as heat. Some of it is spent in suspension of the material in the field of gravity. The dissipated power in this case is approximately equal to the power expended in the initiation of fluidization:

$$N_0 = \Delta p S u_0. \quad (1)$$

The remaining energy of the gas flow is spent in displacing the disperse material in the fluidized bed. The corresponding dissipated power is

$$\Delta N = N - N_0 = \Delta p S (u - u_0). \quad (2)$$

The gas (over and above that required to suspend the material) erupts through the bed in the form of individual gas bubbles, which move with acceleration [4]. Following in the wake of the bubble is a trail of solid particles [9], which accelerate together with it. It is assumed that a gas-flow energy proportional to ΔN is spent per unit time in accelerating the trailing particles.

We derive the volume of a layer of height dx and write the power balance condition:

$$S(u - u_0) dp = l \frac{d}{dt} \left(\frac{u_b^2}{2} \right) dm, \quad (3)$$

for which it is assumed that the energy spent in accelerating the gas, because of the relatively low density of the latter, is negligibly small. Inasmuch as all particles are suspended by the gas flow in a fluidized bed, the equality $dp = \rho g \epsilon dx$ holds. We introduce the quantity k' , which represents the fractional volume occupied by the trails of the moving bubbles in the fluidized layer of height dx . Then the mass of material in the trails is $dm = k' \rho \epsilon S dx$. Relation (3) assumes the form

$$\frac{d}{dt} (u_b^2) = \frac{2g(u - u_0)}{lk'}. \quad (4)$$

Expressing the relationship between dx and dt , i. e., $dt = dx/u_b$, we integrate (4):

A. V. Lykov Institute of Heat and Mass Transfer, Academy of Sciences of the Belorussian SSR, Minsk.
Translated from *Inzhenerno-Fizicheskii Zhurnal*, Vol. 31, No. 2, pp. 323-327, August, 1976. Original article submitted July 10, 1975.

This material is protected by copyright registered in the name of Plenum Publishing Corporation, 227 West 17th Street, New York, N.Y. 10011. No part of this publication may be reproduced, stored in a retrieval system, or transmitted, in any form or by any means, electronic, mechanical, photocopying, microfilming, recording or otherwise, without written permission of the publisher. A copy of this article is available from the publisher for \$7.50.

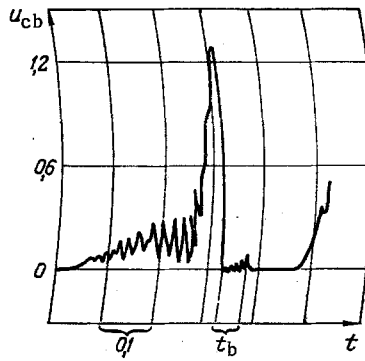


Fig. 1. Typical profile of probe signal during passage of a gas bubble (t_b in sec; u_{cb} in m/sec).

$$\int_{u-u_0}^{u-u_0+v_b} u_b^2 du_b = \frac{g}{k} (u-u_0) \int_0^h dx, \quad (5)$$

whereupon

$$v_b^3 \left[3 \left(\frac{u-u_0}{v_b} \right)^2 + 3 \left(\frac{u-u_0}{v_b} \right) + 1 \right] = \frac{3g}{k} (u-u_0) h. \quad (6)$$

It is known from the two-phase theory of fluidization [9] that

$$\frac{u-u_0}{v_b} = \frac{H}{H_0} - 1. \quad (7)$$

It is clear that for small expansions H/H_0 of the bed and for a sufficient height h terms containing the factor $[(u-u_0)/v_b]^2$ and $(u-u_0)/v_b$ can be neglected. Denoting the bracketed expression in (6) by p' , that expression takes the form

$$v_b^3 = \frac{3g}{p'k} (u-u_0) h. \quad (8)$$

Using the relationship between the relative bubble velocity and diameter [4]

$$v_b \sim \sqrt{gD_b}, \quad (9)$$

we finally obtain

$$D_b = \frac{q}{\sqrt[3]{g}} [(u-u_0) h]^{2/3}, \quad (10)$$

where q is a dimensionless coefficient independent of h and $u-u_0$.

We carried out an experimental investigation to test the foregoing model representations. We conducted the experiments in a column 300 mm in diameter, using two materials: sand ($d = 0.23$ mm, $u_0 = 6$ cm/sec) and silica gel ($d = 0.19$ mm, $u_0 = 2$ cm/sec). The height of the stationary layer was approximately 45 cm in all the experiments. We used a dynamometer probe, the operating principle of which has been described earlier [10]. It comprises a flexible phosphor bronze plate with a rigid needle at the end. A plastic sphere 5.5 mm in diameter is planted on the tip of the needle. The force acting on the sphere is measured with two strain gauges cemented onto the flexible plate and connected to a TA-5 strain-reading instrument. The output signal from the latter is recorded on the strip chart of an N-327-3 high-speed recording unit. The probe is calibrated by weighting the sphere with a static load. The force acting on the probe is determined with 5% error in the frequency range from 0 to 50 Hz. In our experiment we set the probe at two heights from the gas-distributing grid: 20 cm and 40 cm. The probe was installed in the following sequence: first an initial charge of material was poured into the column, then the probe was installed, and finally the remaining material was poured in to bring the total height to 45 cm. The rates of fluidization of the tested materials were determined by the standard procedure (from the pressure difference). The ranges of fluidization numbers were 4 to 6 and 7.5 to 30 for sand and silica gel, respectively.

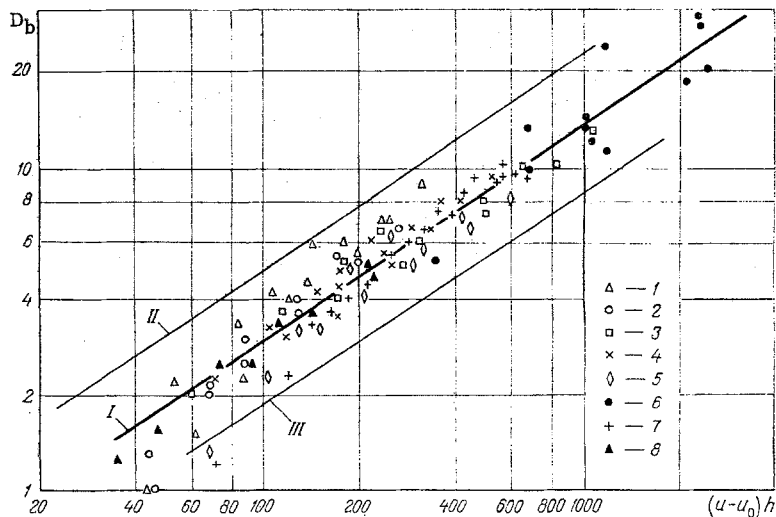


Fig. 2. Bubble diameter D_b , cm, versus product $(u - u_0)h$, cm^2/sec . 1-5) Data of Rowe and Sverett [1] (see Table 1); 6) our data for sand; 7) data of Werther and Molerus [3]; 8) data of Werther and Molerus [11].

The probe was dynamically calibrated by means of motion picture film in a plane column with a cross section 240×35 mm. At the instant of passage of the rear of the bubble the probe signal was recorded and its velocity determined from the motion picture film. The dynamic calibration error did not exceed 5%.

A typical signal plotted by the recording unit during passage of a bubble through the probe sphere is given in Fig. 1. It is evident from the figure that during the transit time t_b of the bubble past the probe the signal is equal to zero, but it increases sharply at the instant the rear of the bubble passes the probe. On the strip chart we measured the length of the zero-signal line and height of the spike after the bubble (rear of the bubble). Then, knowing the strip speed, we determined the bubble transit time past the probe and, using the static and dynamic calibration, obtained the speed of the rear of the bubble. From these data we determined the height of the bubbles in each individual case and the average height, which we took as the bubble diameter D_b .

The experimental points are given in Fig. 2 in logarithmic coordinates of the bubble diameter as a function of the product of the excess velocity of the gas by the height from the gas distributor. Also shown in the same figure are the data of other authors using different procedures for measuring the bubble diameter under different conditions (see Table 1).

All the experimental points are generalized in the given coordinate system within 20% rms error limits by a straight line with a slope of approximately 0.67 (line I):

TABLE 1. Experimental Conditions

Source	Solid particles	u_0 , cm/sec	d , μ	Column, cm	Measurement technique	No. in Fig. 2
[1]	Aluminum	2,54	210	20×30	X rays	2
	Coal	8,0	296			1
	Quartz	2,75	135			3
	Spherical pellets	8,0	323			4
	Glass powder	5,5	268			5
[2]	Glass balls	2,4	120	∅ 7,62 10×10	Capac. probe Capacitance probe + x rays	
	Quartz sand	1,8	100	∅ 10	Capac. probe	
[4]	Silica gel	2,85	150	∅ 10	Photoelectric probe	
[5]	Glass balls	0,72	74	7,5×15	X rays	
[6]	Aluminum catalyst	64,5	1520	61×2 61×5	Explosion diameters (film)	
[7]	Aluminum catalyst	55	1540	30,5×15,2	Explosion diameters (visual)	
[11]	Quartz sand	1,8	83	∅ 100	Capac. probe	

$$D_b = \frac{1.3}{\sqrt[3]{g}} [(u - u_0)h]^{2/3} \quad (11)$$

This equation can be written in the dimensionless form

$$D'_b = 1.5 \sqrt{\text{Fr}^*} \quad (12)$$

Our data for silica gel lie somewhat above the line described by (11), namely, along line II in Fig. 2. The data of another group of researchers [2, 5, 6, 7] are well approximated by lines II and III, which are parallel to the middle line I described by (11). The parallelism of these lines confirms the validity of relation (10) derived above. The parallel displacement (different values of the coefficient q) is apparently attributable to different conditions of bubble formation in the grid zone of the bed (different initial values of the bubble diameter after the gas-distributing grid).

Thus, despite the diverse conditions of bubble growth and behavior in the experiments of different researchers, the bubbles obey common fundamental growth laws, which are represented by Eq. (10). Relation (11) makes it possible to calculate the bubble diameters in equipment using porous grid-plates at distances of 200 mm or more from the gas distributor.

Comparing (11) with the analogous relation obtained by Kobayashi and others [4], we note that the latter better fits the experimental data for $(u - u_0)h \leq 100 \text{ cm}^2/\text{sec}$. In that range, however, the error is large in the determination of D_b . In the interval $100 \leq (u - u_0)h \leq 300 \text{ cm}^2/\text{sec}$ both relations give roughly the same results. In the interval $(u - u_0)h > 300 \text{ cm}^2/\text{sec}$, which is of considerable practical interest, the Kobayashi relation [4] yields results that are clearly too large.

Thus, Eqs. (10) and (11) enable one to calculate the diameters of erupting gas bubbles in industrial fluidized bed equipment.

NOTATION

D_b , bubble diameter; d , particle diameter; $D' = D_b/h$, dimensionless bubble diameter; $\text{Fr}^* = (u - u_0)^2/D_b g$, modified Froude number; g , free-fall acceleration; h , height above grid; H_0 , initial height of bed; H , instantaneous bed height; l, k , proportionality factors; p , gas pressure; Δp , pressure difference in bed; S , column cross section; u_b , absolute bubble velocity; v_b , relative bubble velocity; u_0 , rate of initiation of fluidization; u , gas filtration rate; ρ , material density of particles; ϵ , particle concentration in bed.

LITERATURE CITED

1. P. N. Rowe and D. J. Sverett, *Trans. Inst. Chem. Eng.*, **50** (1972).
2. R. Toei, R. Matsuno, H. Kojima, Y. Nagai, K. Nakagawa, and S. Yu, Reprint from *Mem. Fac. Eng. Kyoto Univ.*, **27**, 4 (1965).
3. J. Werther and O. Molerus, *Internat. J. Multiphase Flow*, **1**, 123-138 (1973).
4. H. Kobayashi, F. Arai, and T. Chiba, *Kagaku Kōgaku*, **4**, No. 1 (1966).
5. P. Baumgarten and R. Pigford, *AIChE J.*, **6**, No. 1 (1959).
6. D. Geldart and R. Cranfield, *Chem. Eng. J.*, **3** (1972).
7. L. McGrath and R. Streatfield, *Trans. Inst. Chem. Eng.*, **49** (1971).
8. R. Cranfield and D. Geldart, *Chem. Eng. Sci.*, **29**, 935-947 (1974).
9. J. F. Davidson and D. Harrison (editors), *Fluidization*, Academic Press, New York (1971).
10. A. I. Tamarin, I. Z. Mats, and G. G. Tyukhai, in: *Heat and Mass Transfer in Disperse Systems* [in Russian], Minsk (1968).
11. J. Werther and O. Molerus, *Chem.-Ing.-Tech.*, **43**, No. 5 (1971).